Excited State and Ground State Proton Transfer Rates of 3-Hydroxyflavone and Its Derivatives Studied by Shpol'skii Spectroscopy: The Influence of Redistribution of Electron Density†

Arjen N. Bader,‡ Vasyl G. Pivovarenko,§ Alexander P. Demchenko,|| Freek Ariese,‡ and Cees Gooijer*,‡

Department of Analytical Chemistry and Applied Spectroscopy, Laser Centre, Vrije Universiteit, De Boelelaan 1083, 1081 HV Amsterdam, The Netherlands, Department of Chemistry, Organic Chemistry Chair, Kiev National Taras Shevchenko University, Kiev 01033, Ukraine, and TUBITAK Research Institute for Genetic Engineering and Biotechnology, Gebze-Kocaeli 41470, Turkey

Received: March 10, 2004; In Final Form: April 27, 2004

We studied the mechanisms of excited-state intramolecular proton transfer (ESIPT) and ground-state back proton transfer (BPT) in 3-hydroxyflavone (3HF) at cryogenic temperatures. The focus was on substituents that change the distribution of electronic density on the chromophore and their influence on these reaction rates. Shpol'skii spectroscopy was applied for comparative studies of three compounds: 3HF, 3-hydroxy-4′-methoxyflavone (3HF-4′OMe), and 2-furyl-3-hydroxychromone (3HC−F). By comparing the spectral bandwidths with those of deuterated analogues, we could distinguish the lifetime broadening components in the high-resolution excitation and emission spectra, from which the time constants of the ESIPT and BPT reactions were calculated. The time constants for the ESIPT reaction were 0.093 ps for 3HF, 0.21 ps for 3HF-4′OMe, and slower than 0.6 ps for 3HC−F. For the same compounds, the BPT rates were 0.21, 0.47, and >2 ps, respectively. No change in bandwidth was observed over the temperature range 4−20 K, in agreement with a tunneling mechanism. Estimates for the barrier heights and proton-transfer distances are given. In addition, a systematic change in O−H bond strengths between ground and excited states was calculated from the isotope effect, observed as the shifts of the 0−0 bands in the excitation and emission spectra upon deuteration. The substantial effect of electron donating substituents on the rates of ESIPT and BPT reactions is in agreement with these changes.

Introduction

3-Hydroxyflavone (3HF; see Scheme 1) is one of the most intensively studied compounds that undergo excited-state intramolecular proton transfer (ESIPT). The unique feature of this molecule is that dual fluorescence emission can be observed: the normal form of the excited state (N*) emits in the blue and the excited-state tautomeric form (T*) in the green.[1−7] Since the rate of ESIPT (and therefore whether blue, green or dual emission is observed) depends on the interaction with the surrounding solvent molecules,[2−7] it can be used as a ratiometric probe.[8−10] Newly synthesized 3HF derivatives exhibit a more significant electronic charge separation in the N* state.[11−13] This allowed us to observe dual emission in low polarity environments and, thus, to extend dramatically the range of two-band ratiometric responses.[14−18] These ratiometric probes based on the 3HF chromophore become more and more functional; they allow efficient sensing at the molecular level of solvent polarity and electronic polarizability,[19] hydrogen bond donor ability,[20] and electrostatic field effects.[21] Their applications range from micelles[22] to proteins[23] and biomembranes and their phospholipid models.[24−28] Meanwhile, one of the fundamental questions remains unanswered: how do these changes in molecular structure influence the basic ESIPT rates? Since in the design of new probes the substitutions are commonly made at sites remote from the groups participating in ESIPT, we hypothesize that the proton transfer barrier heights could be strongly dependent on changes in electronic density in the groups involved. This study on ESIPT and BPT rates as a function of molecular (and primarily, electronic) structure will help us understand the underlying mechanisms and will be useful for the development of new advanced probes based on 3HF.

One of the most recent approaches for studying the ESIPT reaction in 3HF is using Shpol'skii spectroscopy.[29,30] Moreover, the rates of the fast T → N ground-state back proton transfer (BPT) reaction can also be obtained, which is not possible using common time-resolved techniques.[31,32] When embedded in a cryogenic crystalline *n*-octane matrix, no solvent reorganization can take place, and to a good approximation, all guest molecules experience the same solvent/solute interaction. As a result, for many compounds that fit in the Shpol'skii matrix in terms of polarity and geometry, the inhomogeneous broadening can be reduced to ca. 4 cm^{-1}. The idea behind using this approach for measuring proton transfer rates is that in cases where the rate of ESIPT is extremely fast, and therefore the lifetime of the N* state extremely short, additional broadening in the excitation spectrum will be observable. Similarly, additional broadening observed in the emission spectrum will indicate a very short lifetime of the T state caused by the fast BPT reaction. A

† Part of the special issue "Gerald Small Festschrift".

* To whom correspondence should be addressed. E-mail: gooijer@few.vu.nl. Fax: +31-20-4447543. Tel: +31 20 4447540.

‡ Vrije Universiteit.

§ Kiev National Taras Shevchenko University.

|| TUBITAK Research Institute for Genetic Engineering and Biotechnology.

10.1021/jp048925e CCC: $27.50
Published on Web 06/04/2004

SCHEME 1

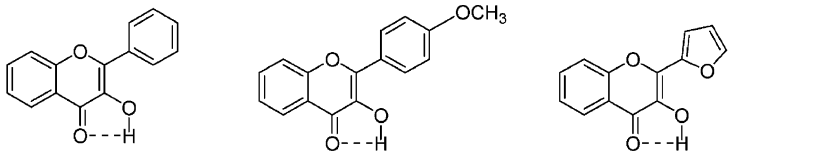

3-hydroxyflavone (3HF) **4'methoxy-3-hydroxyflavone (3HF-4'OMe)** **2-furyl-3-hydroxychromone (3HC-F)**

distinction between the effects of homogeneous (lifetime-dependent) broadening and inhomogeneous broadening (dependent on solvent environment effects) can be made by comparing the Shpol'skii excitation and emission spectra of 3HF and its deuterated analogue 3-deuterioxyflavone (3DF). Excited-state intermolecular deuteron transfer (ESIDT) and back deuteron transfer (BDT) are much slower than ESIPT and BPT, respectively. The longer lifetime of the N* and T states and the insignificant homogeneous broadening contribution to the spectral lines allow us to determine the extent of inhomogeneous broadening in 3DF. Using these values for 3HF (the inhomogeneous broadening for protonated and deuterated compounds will be equal), the contribution from homogeneous broadening can be derived from the total broadening observed in the spectra, and the lifetimes of the N* and T states can be obtained.[29]

Following this approach, it was estimated that ESIPT in 3HF in cryogenic Shpol'skii matrixes takes place in approximately 40 fs.[29] Unfortunately, due to limited data handling possibilities of the CCD camera used in those experiments, the resolution in the excitation dimension was still relatively poor, i.e., no better than 0.5 nm. With our recently improved setup, a kinetic series of a large number of emission spectra can be recorded, as the excitation wavelength of the dye laser is slowly scanned at a constant rate. This has resulted in a much better resolution in the excitation spectrum: in the present setup the resolution is comparable to the one in emission (0.05 nm), which allows us to achieve a much higher precision in the determination of ESIPT rates in the femtosecond time range.

In a previous paper, we studied derivatives of 3HF that contained at the 2-position a π-donor heterocycle with higher electron donor ability than phenyl: furyl, benzofuryl, and naphthofuryl groups.[30] Interestingly, for these derivatives, no broadening due to lifetime effects was observed and we concluded that ESIPT and BPT must take place at the picosecond time scale. Possible reasons for this slower proton transfer in both excited state and ground state are steric effects of the substituents with different geometry or electronic effects caused by a different redistribution of electron density in the molecule. The oxygen in the furyl group might form a hydrogen bond with the 3-hydroxy group, resulting in a geometric effect, i.e., in a longer proton-transfer distance to the carbonyl at the 4-position. As will be shown below, these long proton-transfer distances do not agree with the rates of proton-transfer dealt with. The focus in this paper will therefore be on the electron donating ability of the 2 position of the chromone. An electron donating group at this position may affect the acidity of the 3-hydroxy group and the bond order of the 4-carbonyl group and therefore the basicity of its oxygen atom; both effects will influence the proton-transfer rates.

In this paper, we investigate the dynamics of the ESIPT and BPT processes in 3HF and in two of its derivatives (see Scheme 1) in more detail using Shpol'skii spectroscopy, i.e., besides 3HF and 2-furyl-3-hydroxychromone (3HC−F), also 3-hydroxy-4′-methoxyflavone (3HF-4′OMe). The *p*-methoxy group in the latter compound is known for its electron donating properties, which makes it similar to the furyl-group. However, the *p*-methoxy group is expected to be somewhat less efficient in redistributing the electron density over the chromone moiety than a furyl group is.

The Shpol'skii spectroscopy approach to determine the rates of ESIPT and BPT allows us to study another effect as well. In the Shpol'skii excitation spectra of 3HF and 3DF, an energy difference between their N → N* transitions can be seen.[29] This isotope effect is not expected to be due to changes in the purely electronic $S_0 \rightarrow S_1$ energy difference, since substitution of a proton by a deuteron will not result in significant changes in the electronic structure of the molecule. However, if the strength of the O−H bond changes upon excitation, then the distance between the zero-point energy (ZPE) levels in the ground and excited states will be different for 3-OH and 3-OD derivatives. The observation of such a difference in ZPE for these two isotope species gives direct information about the change in the 3-OH vibrational energy upon excitation and can therefore be used to verify the changes in the acidity or basicity of this group. Similar observations in emission deal with the tautomeric forms of 3HF and 3DF and therefore indicate the changes in vibrational energy of the 4-OH group (formed as a result of ESIPT reaction). We will examine such shifts for 3HF-4′OMe and 3HC−F in order to study the effects of electron donating substituents on the proton-transfer process.

Experimental Section

All measurements were done using 10^{-5} M solutions of 3-hydroxyflavone (Extrasynthèse, Genay, France), 2-furyl-3-hydroxychromone (synthesis described in earlier work[30]), and 3-hydroxy-4′-methoxyflavone (synthesis described below) dissolved in *puriss. n*-octane (Fluka). Deuteration of the flavones was achieved by adding the same volume of D_2O (Aldrich) to a solution of the flavone in octane. After shaking this two-phase system, deuteration of the 3-OH group of the flavone was achieved in 30 min. The upper layer formed is a solution of the deuterated flavone in *n*-octane. Any traces of incomplete deuteration could be clearly distinguished in the Shpol'skii spectra. No additional purification steps were applied to any of the samples. 30 μL of the sample solution was transferred to a 2 mm i.d. quartz tube that was closed with a septum.

3-Hydroxy-4′-methoxyflavone, (3HF-4′OMe) was prepared by alkaline condensation of 4-methoxybenzaldehyde with 2′-hydroxyacetophenone (both purchased from Aldrich) and subsequent oxidative heterocyclization of the obtained chalcone with hydrogen peroxide.[33] Light green-yellow crystals of 3HF-4′OMe were recrystallized twice from a 1% solution of acetic acid in ethanol and dried in a vacuum at 110 °C. The obtained crystals with mp 233−234 °C (231−232 °C[33]) presented a homogeneous product according to ^{1}H NMR and TLC criteria. TLC was run on 50 × 150 mm plates of "Silufol" using 98:2, 95:5, and 9:1 (v/v) chloroform−methanol eluents. Checking for impurities was done under UV illumination at 254 and 356 nm.

The ^{1}H NMR spectrum of 3HF-4′OMe was measured on a Varian Mercury-400 apparatus in DMSO-d_6. The chemical shifts, multiplicities (s, singlet; d, doublet; t, triplet; m, multiplet), and signal intensities (in brackets) were 9.18 s (1H); 8.21 d (2H); 8.10 d (1H); 7.75 t (1H); 7.66 d (1H); 7.41 t (1H); 7.04 d (2H); 3.86 s (3H). The ^{13}C NMR spectrum of 3HF-4′OMe was measured in DMSO-d_6 and showed the following chemical shifts 173.2; 161.0; 155.0; 146.1; 138.7; 134.0; 130.0; 125.3; 125.0; 124.1; 121.9; 118.9; 114.6; 55.9.

Four quartz tubes at a time were placed in a row in a homemade sample holder that was mounted to the top of the cold head of a closed cycle 4 K liquid-helium refrigerator (SRDK-205 Cryocooler, Janis Research Company, Wilmington, MA). The excitation source was a XeCl excimer laser (Lambda Physik LPX 110i, Göttingen, Germany) pumping a dye laser (Lambda Physik, LPD 3002). The excimer laser was operated at 10 Hz, producing 10 ns, 50 mJ pulses. Using DMQ as a dye, a tuneable output in the 340−375 nm range was obtained, while QUI was used to enable excitation in the range from 370 to 400 nm. The four samples could be measured separately by moving the cold head at an angle of 45° with respect to both the excitation and emission beam. Fluorescence emission was collected with a 3 cm F/l.2 quartz lens at a 90° angle to the excitation beam, focused by a 10 cm F/4 quartz lens on the entrance slit of a Spex 1877 0.6 m triple monochromator (Edison, NJ) and detected with an intensified CCD camera (iStar DH720−25U-03, Andor instruments, Belfast, Northern Ireland) operated in the gated mode (delay = 20 ns; gate = 100 ns) to reject stray and scattered light. The spectral resolution of the emission spectrum (limited by the spectrographh/ICCD) was 0.1 nm (4 cm^{-1}).

The excitation spectra were obtained by measuring a kinetic series of emission spectra while the dye laser was scanned at a constant rate. In this study, this rate was 0.05 nm/spectrum. Every 5 s (or 50 pulses of the dye laser), a spectrum was recorded, resulting in an excitation resolution of 2 cm^{-1} with a repeatibility of 0.1 cm^{-1}. The excitation spectra were obtained by plotting the intensity of a T ← T* emission band (three pixels were summed) versus the excitation wavelength. To reduce the noise due to pulse-to-pulse intensity fluctuations, three kinetic series of emission spectra were recorded and averaged. No correction was applied for the wavelength dependency of the intensity of the dye laser nor for the intensity loss due to photodecomposition.

Results and Discussion

The Shpol'skii emission spectra of 3-hydroxy-4′-methoxyflavone (3HF-4′OMe) in *n*-octane matrix recorded at different excitation wavelengths are shown in Figure 1. The spectrum displays many sites, which overlap due to broadening effects (for the deuterated analogue much better resolution was observed, as shown below). As can be seen in this figure, there is one separate site at 519 nm and a cluster of approximately four sites between 520 and 524 nm. We will focus on the separate site to study line broadening effects. The excitation spectra of 3-hydroxyflavone and 2-furyl-3-hydroxychromone (3HC-2F) have been published in earlier work.[29,30] Here, we report the improved spectra recorded under better instrumental resolution conditions.

The laser excited Shpol'skii excitation and emission spectra of all compounds (recorded using the same setup) are shown in Figures 2 and 3, respectively. Because the focus is on bandwidths, only the (0,0) region of the major site is shown for each compound. As regards the line positions, for the deuterated compounds, the major sites are found at excitation and emission wavelengths that differ from those of the nondeuterated compounds. In excitation, the bands of the deuterated compounds are blue shifted, whereas in emission, they are redshifted; this will be discussed in more detail below. Nonetheless, apart from the bandwidth, the site structures observed for the deuterated and the nondeuterated compounds are equal, confirming that the fit of the studied compounds in the *n*-octane matrix is not changed by deuteration. The estimation of the excitation bandwidth Γ_{exc} from Figure 2 is much more accurate than that presented in earlier work,[29,30] because of the smaller 0.05 nm scan steps applied. It should be emphasized that this improvement is not due to the lower sample temperature applied in the new setup; when the new cryostat was set at 11 K instead of 4 K, identical excitation spectra were observed.

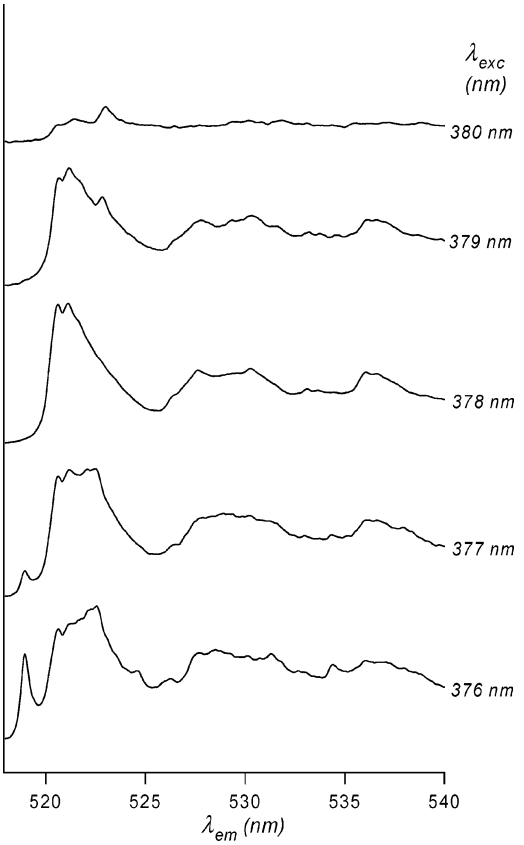

Figure 1. 4 K Shpol'skii emission spectra of 3HF-4′OMe in *n*-octane, recorded at different excitation wavelengths.

Considering the three compounds in Figures 2 and 3, the bandwidths both in the excitation and in the emission spectra decrease in the order: $\Gamma_{3HF} > \Gamma_{3HF-4'OMe} > \Gamma_{3HC-2F}$. From these bandwidths, the lifetimes of the N* and T states can be calculated following the procedure outlined before.[29] The assumption that for the deuterated compounds the (deuteron) transfer rates are too low to cause observable homogeneous broadening is crucial. The results are presented in Table 1. The calculated lifetimes of the N* and T state correspond to the rates of fast ESIPT and BPT, respectively.

Table 1 reveals that the differences between the ESIPT and BPT rates of 3HF and 3HF-4′OMe are similar and relatively small, they differ by only a factor of 2.2. For 3HC-2F, this regularity cannot be verified because the ESIPT and BPT rates are too slow to induce measurable line width changes. More interesting are the differences in ESIPT rates between the studied compounds. In 3HF-4′OMe compared to 3HF, the ESIPT is slower by only a factor of 2. ESIPT in 3HC-2F is much slower,

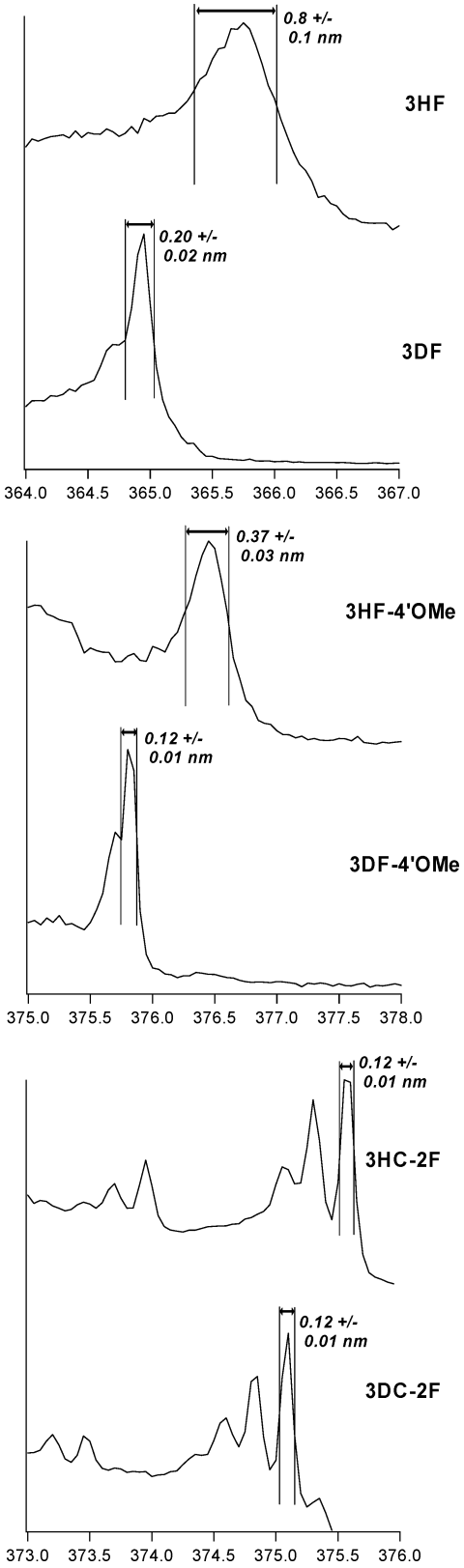

Figure 2. 4 K Shpol'skii excitation spectra (0,0 regions, nanometers) of 3HF, 3HF-4′OMe and 3HC−F and their deuterated analogues. The wavelengths of emission are given in Table 3. From the indicated values of the bandwidth, the rates of ESIPT are calculated (listed in Table 1).

i.e., more than 6 times compared to 3HF. These slower time constants observed for 3HF-4′OMe and 3HC−F are expected to be due to the increase of electronic density located on the γ-pyrone ring of the molecule: stronger electron donating groups at the 2-position will result in a slower ESIPT reaction.

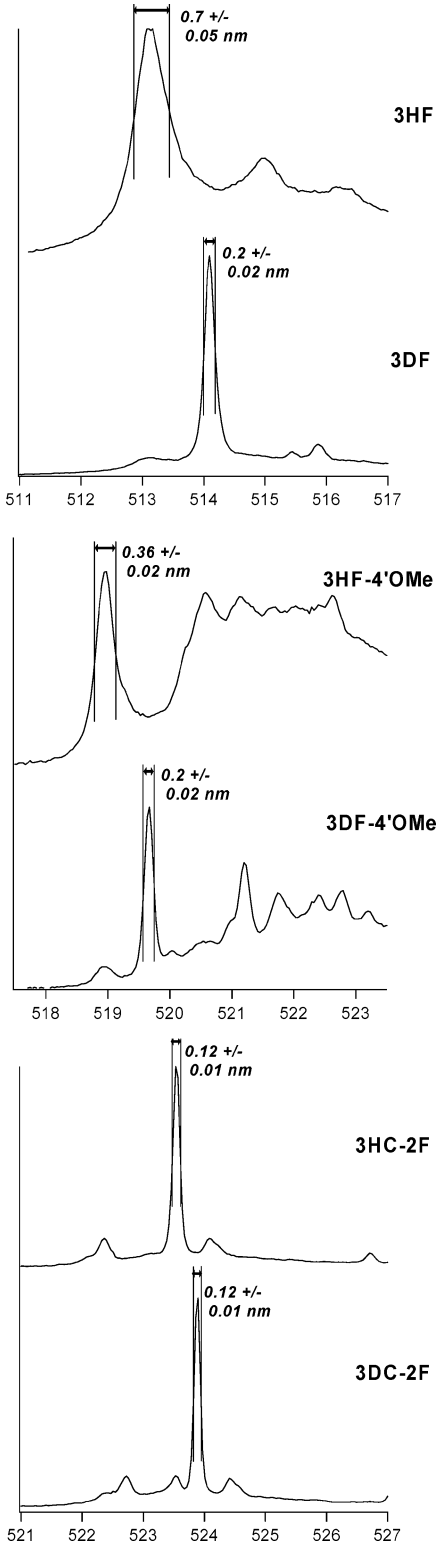

Figure 3. 4 K Shpol'skii emission spectra (0,0 regions, nanometers) of 3HF, 3HF-4′OMe, and 3HC−F and their deuterated analogues. The wavelengths of excitation are given in Table 3. From the indicated values of the bandwidth, the rates of BPT are calculated (listed in Table 1).

The observed spectral bandwidths, and therefore the proton-transfer rates, were found to be temperature independent over a 4−20 K temperature range (not shown). This observation rules out thermal activation as the mechanism of proton transfer at low temperatures. Combined with the observed large differences between ESIPT and ESIDT (and similarly between BPT and BDT) rates, the conclusion can be drawn that tunneling is the

TABLE 1: Rates of Excited-State Intramolecular Proton Transfer (ESIPT) and Back Proton Transfer (BPT) Determined for 3HF and Its Derivatives[a]

	Γ_{tot} (cm^{-1})		Γ_{instr}	Γ_{inh} (cm^{-1})		Γ_{hom} (cm^{-1})		
	min.	max.	(cm^{-1})	min.	max.	min.	max.	τ_{pt} (ps)
				3HF				
ESIPT	52	67	4	0	16	50	67	0.093 ± 0.01
ESIDT	14	17	4	0	16	0	16	>0.3
BPT	24	28	4	0	7.3	23	28	0.21 ± 0.02
BDT	6.7	8.2	4	0	7.3	0	7.3	>0.7
				3HF-4′OMe				
ESIPT	24	29	4	0	8.3	22	29	0.21 ± 0.03
ESIDT	7.8	9.2	4	0	8.3	0	8.3	>0.6
BPT	12	14	4	0	7.2	10	14	0.47 ± 0.08
BDT	6.7	8.2	4	0	7.2	0	7.2	>0.7
				3HC-2F				
ESIPT	7.8	9.2	4	0	8.3	0	8.3	>0.6
ESIDT	7.8	9.2	4	0	8.3	0	8.3	>0.6
BPT	4.0	4.7	4	0	2.5	0	2.5	>2
BDT	4.0	4.7	4	0	2.5	0	2.5	>2

[a] The rate of ESIPT is obtained from the total bandwidths of the site-selected band in the excitation spectra (see Figure 2). The rate of BPT was obtained from the total bandwidth of the site-selected band in the emission spectra (see Figure 3). The homogeneous broadening (Γ_{hom}) was calculated from the total broadening (Γ_{tot}), the instrumental broadening (Γ_{instr}), and the inhomogeneous broadening (Γ_{inh}) via $\Gamma_{tot}^2 = \Gamma_{instr}^2 + \Gamma_{inh}^2 + \Gamma_{hom}^2$.

most likely mechanism of proton (and deuteron) transfer. Of course at higher temperatures, thermally activated processes will become more significant.

In an oversimplified way, tunneling in a proton-transfer reaction can be described using a one-dimensional semiclassical model.[34−36] In this model, a parabolic barrier is used with width R (proton-transfer distance) and height ΔE (maximum barrier height above the ZPE) as parameters. Under these constraints, the rate of proton tunneling (k_H) obeys the following equation:

$$k_H = \nu_H \exp[-(\pi^2/h)R(2m_H\Delta E)^{1/2}] \quad (1)$$

wherein h is Planck's constant, m_H is the proton mass, and ν_H is the vibrational frequency along the proton-transfer reaction coordinate. For the 3HF derivatives dealt with in the present study, an estimation of ν_H cannot be easily made. This is due to the fact that the proton will presumably not be transferred exactly in the same direction as the OH-group's vibrational motions. The proton transfer coordinate will predominantly be determined by the OH stretching component, but the OH bending component and some (skeleton) vibrations may also be involved. To estimate the corresponding barrier heights according to the simple model of eq 1, $\nu_H = 3500$ cm^{-1} was used. The resulting values of $R(\Delta E)^{1/2}$ and the values of ΔE (for a distance $R = 0.2$ and 0.4 Å) are given in Table 2.

For further analysis, it is assumed that the proton-transfer distances (i.e., the barrier widths) for 3HF and 3HF-4′OMe are equal, an assumption that seems quite reasonable in terms of molecular structures of these compounds. It should be noted that, although the calculated barrier heights are very low (especially when $R = 0.4$ Å), because of the low temperatures dealt with they are still higher than the activation energies. It was observed that 3HF-4′OMe shows a two times lower ESIPT rate (and BPT rate) than 3HF. Assuming that the barrier widths are equal for the three compounds, this implies that upon methoxy substitution at the 4′ position the barrier height increases with a factor of 1.9; it should be noticed that this outcome is independent of the proton-transfer distance. Similarly, for 3HC−F, a reduction in proton-transfer rates − at least 6 times slower in comparison to 3HF − was observed. Therefore, the barrier height is thought to be enhanced at least 3.4 times upon substitution of the phenyl group in 3HF by a furyl group.

Equation 1 can also be used for a crude approximation of the rate of ESIDT (k_D); incorporation of deuteron mass m_D, vibrational frequency ν_D ($= 2^{-1/2}\nu_H$), and ΔE_D ($= \Delta E_H - ZPE_H + ZPE_D$) results in a one order decrease in the transfer rate when $R = 0.2$ Å and almost two order decrease in the transfer rate when $R = 0.4$ Å. This agrees with the results presented here: ESIDT should be slower than 0.5 ps (no additional homogeneous broadening in the excitation spectrum was observed), but significantly faster than the blue emission from the N* state (≈1 ns), since such an emission is not observed. For 3HC−F, this means that the time constant for ESIPT is in the low picosecond range, since also its deuterated analogue is emitting in the green (again no blue emission was observed) and therefore has a sub nanosecond ESIDT time constant. Furthermore, as mentioned in the Introduction, H-bond formation between the 3-OH/3-OD group and the oxygen of the furyl group seems highly unlikely. In that case, the barrier width would increase to more than 1.5 Å, resulting in an isotope effect of more than 5 orders of magnitude. This is in disagreement with the experiment.

Interestingly, the N→N* transitions for all of the three compounds are blue shifted upon deuteration. As mentioned in the Introduction, this can be explained by a difference in ZPE. When the strength of the O−H vibration changes upon excitation, the ZPE of the electronic ground state is not equal to the ZPE in the excited state, and a shift in the (0,0) transition energy upon deuteration can be expected, as illustrated in Figure 4. When comparing the ZPEs of the normal forms of 3HF and 3DF, only the contribution of the 3-OH vibrations to the total ZPE needs to be considered since to a good approximation the other molecular vibrations will not be affected. Upon deuteration, the difference in reduced mass is approximately a factor of 2, so that the ZPE in 3HF has to be multiplied by $2^{-1/2}$ to obtain the value of the ZPE of 3DF. Therefore, from the (0,0) energy difference in excitation between 3HF and 3DF, the difference in ZPE between the ground ($ZPE_{H,N}$) and first excited (ZPE_{H,N^*}) state can be calculated using

$$ZPE_{H,N} - ZPE_{H,N^*} = (1 - 2^{-1/2})^{-1}(\Delta E_H - \Delta E_D) = 3.414(\Delta E_H - \Delta E_D) \quad (2)$$

as illustrated in Figure 4. In eq 2, ΔE_H and ΔE_D are the observed (0,0) transition energies for the protonated and deuterated

TABLE 2: Calculated Values for the Barrier in the ESIPT Reaction using eq 1[a]

	ν_H (cm^{-1})	τ_{ESIPT} (ps)	$R(\Delta E)^{1/2}$ (Å(J/mol)$^{1/2}$)	ΔE ($R = 0.2$ Å) (kJ/mol)	ΔE ($R = 0.4$ Å) (kJ/mol)	$\Delta E/\Delta E_{3HF}$
3HF	3500	0.093	20.6	10.5	2.6	1
3HF-4′OMe	3500	0.21	27.9	19.9	5.0	1.9
3HC−F	3500	> 0.6	>38	>36	>9.0	>3.4

[a] For the vibrational frequency ν_H a value of 3500 cm^{-1} was chosen for all compounds.

TABLE 3: Wavelengths of the Main Sites in the Shpol'skii Excitation and Emission Spectra[a]

	λ_{exc} (nm)	$\Delta E_H - \Delta E_D$ (cm^{-1})	$ZPE_{H,N} - ZPE_{H,N^*}$ (cm^{-1})	λ_{em} (nm)	$\Delta E_H - \Delta E_D$ (cm^{-1})	$ZPE_{H,T} - ZPE_{H,T^*}$ (cm^{-1})
3HF	365.75	60	205	513.14	−36	−123
3DF	364.95			514.09		
3HF-4′OMe	376.45	44	150	518.95	−27	−91
3DF-4′OMe	375.82			519.67		
3HC−F	375.60	34	116	523.55	−13	−44
3DC−F	375.12			523.90		

[a] For every compound, the difference between λ_H and λ_D is used to calculate the difference in ZPE, both for the normal form and the tautomeric form.

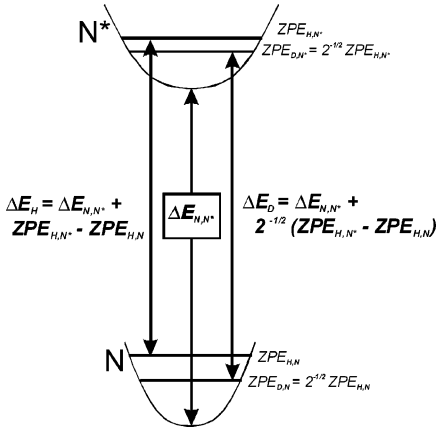

Figure 4. ZPE levels of the protonated compound (subscript index "H") and deuterated compound (subscript index "D") in ground-state N and excited-state N*. Energy differences ΔE_H and ΔE_D are the measured values obtained from the (0,0) bands in the Shpol'skii excitation spectrum. Combining the equation for ΔE_H and ΔE_D results in eq 2.

compound, respectively. Since only the 3-OH group is deuterated, the change in ZPE between ground and first excited state will be the net result of the changes in the three OH-group vibrations (one stretching and two bending modes). Similarly, the change in ZPE can be calculated for the T* → T transition from the (0,0) bands in the emission spectra.

In Table 3, the values of ($ZPE_{H,N} - ZPE_{H,N^*}$) and ($ZPE_{H,T} - ZPE_{H,T^*}$) are given for the three compounds studied here. In excitation, the blue shift indicates that the difference in ZPE, and therefore the energies of the three O−H vibrations, decrease upon going from the N state to the N* state. This indicates a weakening of the O−H bond. Similarly, the red-shift of the (0,0) transition observed in the emission spectra upon deuteration implies a decrease of the difference in ZPE between protonated and deuterated derivatives after the T ← T* transition. This indicates that the 4-OH group formed as the result of ESIPT is weakened if T ← T* takes place. Both effects can be readily conceived: the OH bond becomes less strong before proton transfer is taking place. This explains the observed fast ESIPT (N* → T*) in the excited state and the fast BPT (T → N) in the ground state.

Interestingly, by comparing the magnitude of the changes in ZPE found for the three compounds, the largest O−H weakening is observed for 3HF, the compound with the highest proton-transfer rates, and the smallest effect is observed for the compound with the lowest proton-transfer rates, 3HC−F. The weakening of the OH bond in the N* state means an increase in the acidity of this group, which may explain the fast ESIPT. In presence of an electron donating group at the chromone's 2-position, there is a smaller increase in the acidity of the 3-OH group, resulting in a lower ESIPT rate. Similarly for the BPT reaction, the weakening of the O−H bond at the 4-position in the T state compared to the T* state implies that the acidity of this group becomes higher in the ground state. Consequently, the weakening of the O−H bond will increase the C−O bond order at the 4 position. This explains the high rate of BPT in 3HF. Electron donating substituents in 3HF-4′OMe and 3HC−F, however, will reduce both effects and therefore cause a reduced BPT rate.

It can be concluded that the electron donating substituents have a strong influence on the proton tunneling rates of 3HF and its derivatives. They can significantly reduce the rate of both ESIPT and BPT. These results will help us understand the photophysical behavior of this important class of compounds.

Acknowledgment. A.P.D. acknowledges the "ULTRA" program of the European Science Foundation for the travel grant to Amsterdam. A. V. Turov is acknowledged for providing the NMR spectra.

References and Notes

(1) Sengupta, P. K.; Kasha, M. *Chem. Phys. Lett*. **1979**, *68*, 382−385.
(2) Woolfe, G. J.; Thistlethwaite, P. J. *J. Am. Chem. Soc*. **1981**, *103*, 6916−6923.
(3) Itoh, M.; Tokumura, K.; Tanimoto, Y.; Okada, Y.; Takeuchi, H.; Obi, K.; Tanaka, I. *J. Am. Chem. Soc.* **1982**, *104*, 4146−4150.
(4) Strandjord, A. J. G.; Courtney, S. H.; Friedrich, D. M.; Barbara, P. F. *J. Phys. Chem.* **1983**, *87*, 1125−1133.
(5) McMorrow, D.; Kasha, M. *J. Phys. Chem.* **1984**, *88*, 2235−2243.
(6) Strandjord, A. J. G.; Barbara, P. F. *J. Phys. Chem.* **1985**, *89*, 2355−2361.
(7) Brucker, G. A.; Kelley, D. F. *J. Phys. Chem.* **1987**, *91*, 2856−2861.
(8) Sytnik, A.; Gormin, D.; Kasha, M. *Proc. Natl. Acad. Sci. U.S.A.* **1994**, *91*, 11968−11972.
(9) Sarkar, M.; Ray, J. G.; Sengupta, P. K. *Spectrochim. Acta A* **1996**, *52*, 275−278.
(10) Guharay, J.; Sengupta, B.; Sengupta, P. K. *Proteins* **2001**, *43*, 75−81.
(11) Swiney, T. C.; Kelley, F. D. *J. Chem. Phys.* **1993**, *99*, 211−221.
(12) Chou, P. T.; Martinez, M. L.; Clements, J. H. *J. Phys. Chem.* **1993**, *97*, 2618−2622.
(13) Ormson, M. S.; Brown, R. G.; Vollmer, F.; Rettig, W. *J. Photochem. Photobiol*. **1994**, *81*, 65−72.
(14) Demchenko, A. P.; Klymchenko, A. S.; Pivovarenko V. G.; Ercelen, S. In *Fluorescence Spectroscopy, Imaging and Probes − New Tools in Chemical, Physical and Life Sciences*; Kraayenhof, R., Visser, A. J. W. G., Gerritsen, H. C., Eds.; Springer Series on Fluorescence Methods and Applications; Springer-Verlag: Heidelberg, Germany, 2002; Vol. 2, pp 101−110.
(15) Klymchenko, A. S.; Ozturk, T.; Pivovarenko, V. G.; Demchenko, A. P. *Can. J. Chem.* **2001**, *79*, 358−363.
(16) Klymchenko, A. S.; Ozturk, T.; Pivovarenko, V. G.; Demchenko, A. P. *Tetrahedron Lett.* **2001**, *42*, 7967−7970.
(17) Ercelen, S.; Klymchenko, A. S.; Demchenko, A. P. *Anal. Chim. Acta* **2002**, *464*, 273−287.
(18) Klymchenko, A. S.; Pivovarenko, V. G.; Ozturk, T.; Demchenko, A. P. *New J. Chem*. **2003**, *27*, 1336−1343.
(19) Klymchenko, A. S.; Demchenko, A. P. *Phys. Chem. Chem. Phys.* **2003**, *5*, 461−468.
(20) Klymchenko, A. S.; Pivovarenko, V. G.; Demchenko, A. P. *J. Phys. Chem. A* **2003**, *107*, 4211−4216.
(21) Klymchenko, A. S.; Demchenko, A. P. *J. Am. Chem. Soc.* **2002**, *124*, 12372−12379.

(22) Klymchenko, A. S.; Demchenko, A. P. *Langmuir* **2002**, *18*, 5637−5639.
(23) Ercelen, A. S.; Klymchenko, A. S.; Demchenko, A. P. *FEBS Lett.* **2003**, *538*, 25−28.
(24) Bondar, O. P.; Pivovarenko, V. G.; Rowe, E. S. *Biochim. Biophys. Acta* **1998**, *1369*, 119−130.
(25) Dennison, S. M.; Guharay, J.; Sengupta, P. K. *Spectrochim. Acta A* **1999**, *55*, 1127−1132.
(26) Duportail, G.; Klymchenko, A. S.; Mely, Y.; Demchenko, A. P. *FEBS Lett.* **2001**, *508*, 196−200.
(27) Klymchenko, A. S.; Duportail, G.; Ozturk, T.; Pivovarenko, V. G.; Mély, Y.; Demchenko, A. P. *Chem. Biol.* **2002**, *9*, 1199−1208.
(28) Klymchenko, A. S.; Duportail, G.; Mely, Y.; Demchenko, A. P. *Proc. Natl. Acad. Sci. U.S.A.* **2003**, *100*, 11219−11224.
(29) Bader, A. N.; Ariese, F.; Gooijer, C. *J. Phys. Chem. A* **2002**, *106*, 2844−2849.
(30) Bader, A. N.; Pivovarenko, V. G.; Demchenko, A. P.; Ariese, F.; Gooijer, C. *Spectrochim. Acta A* **2003**, *59*, 1593−1603.
(31) Schwarz, B. J.; Peteanu, L. A.; Harris, C. B. *J. Phys. Chem. A* **1992**, *96*, 3591−3598.
(32) Ameer-Beg, S.; Ormson, S. M.; Brown, R. G.; Matousek, P.; Towrie, M.; Nibbering, E. T. J.; Foggi, P.; Neuwahl, F. V. R. *J. Phys. Chem. A* **2001**, *105*, 3709−3718.
(33) Smith, M. A.; Neumann, R. M.; Webb, R. A. *J. Heterocyclic Chem.* **1968**, *5*, 425−426.
(34) Yu, W.-S.; Cheng, C.-C.; Chang, C.-P.; Wu, G.-R.; Hsu, C.-H.; Chou, P.-T. *J. Phys. Chem. A* **2002**, *106*, 806−8012.
(35) Douhal, A.; Lahmani, F.; Zewail, A. H. *Chem. Phys*. **1996**, *207*, 477−498.
(36) Bell, R. P. *The tunnel effect in chemistry*; Chapmann and Hall: New York, 1980; Chapter 2.